



**HAL**  
open science

## Multi-Scale Modeling and Simulation Flow for Oscillatory Neural Networks for Edge Computing

Stefania Carapezzi, Corentin Delacour, Gabriele Boschetto, Elisabetta Corti,  
Madeleine Abernot, Ahmed Nejim, Thierry Gil, Siegfried Karg, Aida  
Todri-Sanial

► **To cite this version:**

Stefania Carapezzi, Corentin Delacour, Gabriele Boschetto, Elisabetta Corti, Madeleine Abernot, et al.. Multi-Scale Modeling and Simulation Flow for Oscillatory Neural Networks for Edge Computing. NEWCAS 2021 - 19th IEEE International New Circuits and Systems Conference, Jun 2021, Toulon, France. 10.1109/NEWCAS50681.2021.9462761 . lirmm-03197160

**HAL Id: lirmm-03197160**

**<https://hal-lirmm.ccsd.cnrs.fr/lirmm-03197160>**

Submitted on 22 Sep 2021

**HAL** is a multi-disciplinary open access archive for the deposit and dissemination of scientific research documents, whether they are published or not. The documents may come from teaching and research institutions in France or abroad, or from public or private research centers.

L'archive ouverte pluridisciplinaire **HAL**, est destinée au dépôt et à la diffusion de documents scientifiques de niveau recherche, publiés ou non, émanant des établissements d'enseignement et de recherche français ou étrangers, des laboratoires publics ou privés.

# Multi-Scale Modeling and Simulation Flow for Oscillatory Neural Networks for Edge Computing

1<sup>st</sup> Stefania Carapezzi

*Microelectronics Department*  
*LIRMM, Univ. of Montpellier, CNRS*  
Montpellier, France  
ORCID: 0000-0002-9271-1189

2<sup>nd</sup> Corentin Delacour

*Microelectronics Department*  
*LIRMM, Univ. of Montpellier, CNRS*  
Montpellier, France  
Email: corentin.delacour@lirmm.fr

3<sup>th</sup> Gabriele Boschetto

*Microelectronics Department*  
*LIRMM, Univ. of Montpellier, CNRS*  
Montpellier, France  
ORCID: 0000-0001-8830-3572

4<sup>th</sup> Elisabetta Corti

*Dep. of Science and Technology*  
*IBM Research–Zurich*  
Ruschlikon, Switzerland  
ORCID: 0000-0003-4578-7639

5<sup>th</sup> Madeleine Abernot

*Microelectronics Department*  
*LIRMM, Univ. of Montpellier, CNRS*  
Montpellier, France  
Email: madeleine.abernot@lirmm.fr

6<sup>th</sup> Ahmed Nejim

*Silvaco Europe*  
Cambridge, UK  
Email: ahmed.nejim@silvaco.com

7<sup>th</sup> Thierry Gil

*Microelectronics Department*  
*LIRMM, Univ. of Montpellier, CNRS*  
Montpellier, France  
Email: thierry.gil@lirmm.fr

8<sup>th</sup> Siegfried Karg

*Dep. of Science and Technology*  
*IBM Research–Zurich*  
Ruschlikon, Switzerland  
ORCID: 0000-0001-9873-2717

9<sup>th</sup> Aida Todri-Saniai

*Microelectronics Department*  
*LIRMM, Univ. of Montpellier, CNRS*  
Montpellier, France  
ORCID: 0000-0001-8573-2910

**Abstract**—An oscillatory neural network (ONN) is a neuromorphic computing paradigm based on encoding of information into the phases of oscillators. In this paper we present an ONN whose elemental unit, the “neuron”, is implemented through a beyond-CMOS device based on vanadium dioxide (VO<sub>2</sub>). Such ONN technology provides ultra-low power solutions for performing pattern recognition tasks, and it is ideally suited for edge computing applications. However, exploring the groundwork of the beyond-CMOS ONN paradigm is mandatory premise for its industry-level exploitation. Such foundation entails the building of a holistic simulation flow from materials and devices to circuits, to allow assessment of ONN performance. In this work we report results of this advanced designing approach with special focus over the VO<sub>2</sub> oscillator. This establishes the ground to scale up to evaluate beyond-CMOS ONN functionalities for pattern recognition.

**Index Terms**—Oscillatory neural networks (ONN), density functional theory (DFT), technology computer aided design (TCAD), circuit simulation, Internet-of-Things (IoT), edge artificial intelligence (edge AI), neuromorphic computing.

## I. INTRODUCTION

Systems of biological neurons can be mimicked by neural networks, with the neurons emulated after the McCulloch–Pitts [1] or “integrate and fire” [2] models. However, neural systems can be modeled also as periodic oscillators. For instance, features of the visual system are reproduced via nonlinear oscillatory network. In last years, a novel neuromorphic architecture has been suggested [3] based on an ensemble

of coupled oscillators. In such oscillatory neural networks (ONNs) the information is hold by the phases of the oscillators. The coupling laws among the oscillators determine the phase relations among them. It has been demonstrated that the ONNs work as Hopfield neural networks with limit cycles as attractors [3]. Thus, the phase-locked synchronized states yield the outcome of the ONN computation.

A Hopfield neural network realizes a “memory” that can be addressed by content, similarly to the biological associative memory. In this respect, it can perform pattern recognition, which is pivotal for edge artificial intelligence (AI)’s applications, such as surveillance or autonomous driving. By edge AI is meant the evolution of AI of bringing data processing the closest to the location where data are collected, that is our smart devices at the edge of the Internet-of-Things (IoT). The goal is to perform the data analysis at the user’s level, differently to what happens in cloud computing where data have to be sent across Internet. Applications of edge AI pose a serious constrain over power consumption, given that edge devices possess reduced power resources. ONN presents an alternative paradigm that is suitable for computing at the edge due to its low power computing capability. For instance, the embedding of information into oscillator’s phase is a power-saving solution compared to its encoding into oscillator’s amplitude. Also, ONNs have demonstrated fast operation speed that makes them ideally suited for real-time data processing.

In this work we present an innovative implementation of the ONN paradigm to target ultra-low power neuromorphic

This work was supported by the European Union’s Horizon 2020 research and innovation programme, EU H2020 NEURONN (www.neuronn.eu) project under Grant 871501.

computing at the edge. We explore beyond-CMOS devices based on vanadium dioxide ( $\text{VO}_2$ ) for the realization of the fundamental block of the ONN architecture, the oscillator emulating the neuron. The capability of optimizing an ONN architecture with respect to its functionalities is a mandatory step towards the industrial exploitation of this technology. In this context, the assessment of the ONN dynamics and phase-locking synchronization is a necessary premise. In literature, the ONN concept is mainly discussed in terms of mathematically abstract models [5]. Here, we provide an exploratory design flow from materials and devices to circuit-level to enable ONN performance and power assessment. Then, the setting-up of an advanced design toolbox dedicated to beyond-CMOS ONN is an important first step toward achieving technological maturity. This advanced simulation toolchain will encompass all the aspects of interest of the beyond-CMOS ONN, from materials (through atomistic simulations) to devices (by means of technology-computer-aided-design, TCAD) up to circuits (simulations performed through mixed-mode approach and compact models). In this paper, we report the results obtained from such simulation flow with the focus on investigating the beyond-CMOS oscillator (Fig.1). The simulation flow serves as the exploratory toolbox to scale up ONN circuit level description and evaluate its performance on the pattern recognition task.

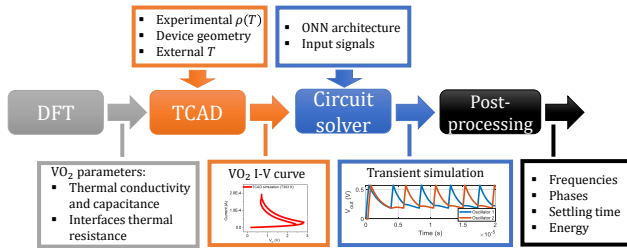


Figure 1. Advanced design toolbox for the simulation workflow of the  $\text{VO}_2$  oscillator.

## II. $\text{VO}_2$ NEURON

### A. Material

Among the transition metal oxides (TMOs),  $\text{VO}_2$  has attracted interest because its phase transition occurs near room temperature ( $\sim 340$  K). It causes a remarkable change in its physical properties, and in particular the material's resistivity varies up to 5 orders of magnitude within a temperature window of 0.1 K for pristine  $\text{VO}_2$ . Furthermore, the phase transition is reversible, and often shows hysteretic behavior. Such low-temperature, ultrafast, and reversible switching is a technological advantage over “traditional” TMOs, and enables the use of  $\text{VO}_2$  for ultrafast memory switches and memory devices.

From a structural perspective, above 340 K  $\text{VO}_2$  has a tetragonal rutile-like (R) crystal structure where the distance between V atoms along the  $c$  axis is constant throughout the lattice, and is 2.96 Å. Notably, R- $\text{VO}_2$  shows metallic behavior

with zero band gap. However, when  $\text{VO}_2$  undergoes its phase transition a distortion in the lattice occurs, and V atoms dimerize with long (3.12 Å) and short (2.65 Å) distances. This breaks the crystal symmetry, and causes a shift to the monoclinic (M1) structure with non-vanishing band gap. This is commonly referred to as metal-to-insulator transition (MIT).

The vast majority of theoretical studies on  $\text{VO}_2$  is about the mechanism leading to the MIT that is now believed to be a cooperative Mott-Peierls [6]. However, significantly less studied is the interaction between  $\text{VO}_2$  and the metal electrode in a typical device architecture, which can provide useful insights into device-level properties. Atomistic simulations of this kind are challenging, as one has to explicitly construct the  $\text{VO}_2$ /metal interface geometry, and thus investigating the different possible surface terminations of  $\text{VO}_2$  becomes pivotal. Furthermore, an in-depth understanding of  $\text{VO}_2$  surfaces is also relevant in order to explore grain boundaries, as it has been observed that the strain caused by the lattice mismatch is able to affect the properties of the MIT, such as the transition temperature and the hysteresis window [7].

In this regard, a limited number of density functional theory (DFT) studies are available in the literature: for instance, focusing on the insulating phase, DFT simulations were carried out on the monoclinic  $\text{VO}_2$  (011) surface in order to compute its electronic properties for catalytic applications [9]. The effect of doping on  $\text{VO}_2$  surfaces has also been explored [7], and results suggest that tuning the material's work function by doping could correlate with a change in the transition temperature.

Ultimately, the aim of our atomistic simulations is to bridge the gap between material's and device properties by constructing  $\text{VO}_2$ /metal interface models that will enable the prediction of relevant material- (band gap, work function) and device-level parameters (e.g., type of contact, interface thermal resistance) that will be fed in subsequent TCAD simulations.

### B. TCAD simulation of Two-Terminal Device

TCAD has been a powerful propellant for the pathway to success of the silicon semiconductor technology. Nonetheless, the mainstream trends of device development (extreme miniaturization, beyond-Si materials) are currently defying the traditional TCAD models. In particular, in case of  $\text{VO}_2$ , its temperature-induced phase change lies outside the standard semiconductor physics commonly provided by TCAD tools. For this reason, the electrical transport in  $\text{VO}_2$  is usually emulated by modeling it as a resistor network [11], and results on TCAD simulations of  $\text{VO}_2$  devices are essentially missing as yet.

We present a TCAD approach suitable to cope with the resistive switching of  $\text{VO}_2$ . To this aim, we customize the Phase Change Material (PCM) model available in Silvaco Victory Device TCAD tool [12]. This model is developed for phase change (PC) materials that pass from crystalline (low resistivity  $\rho$ ) to amorphous state (high  $\rho$ ) depending on  $T$ . PC materials are stable in crystalline/amorphous phase for  $T$  lower/higher than the critical temperatures  $T_{C,\text{cryst}}/T_{C,\text{am}}$ ,

thus therein  $\rho = \rho_{\text{cryst}}/\rho = \rho_{\text{am}}$ . In Silvaco TCAD tools PC materials are modeled as conductors whose local  $\rho$  is made dependent from local  $T$  through the PCM model. The hysteresis of experimental  $\rho$  vs  $T$  curves is accounted for through the Johnson-Mehl-Avrami model.

PC materials and VO<sub>2</sub> show similar behavior of  $\rho$  with  $T$ . However, the PCM model has to be adapted to simulate VO<sub>2</sub>, because  $\rho$  depends on  $T$  also when VO<sub>2</sub> is in semiconducting phase ( $T < T_{C, \text{IMT}, L}$ ). We use a dedicated c-function to customize the PCM model and implement such behavior. We also introduce a  $T$ -dependence of the  $\rho$  for  $T > T_{C, \text{IMT}, H}$  when VO<sub>2</sub> is in metallic phase, in agreement with experimental findings.

We use the customized PCM model to simulate experimental current vs voltage ( $I - V$ ) characteristics of a VO<sub>2</sub> device. This device consists of a VO<sub>2</sub> layer on top of a silicon dioxide substrate (Fig. 2d). The external heater which heats the device at 315.7 K is emulated as thermal boundary condition at the bottom part of the insulator. In VO<sub>2</sub> devices the resistive switching occurs while the current flows across the device. We use the PCM model for VO<sub>2</sub> and we perform electrothermal simulation to investigate the role of self-heating over the resistive change of VO<sub>2</sub>. Fig. 2a shows the good match achieved between simulated (blue line) and experimental (cyan symbols) data. This is a validation of our customized PCM approach to simulate a VO<sub>2</sub> device. Also, it supports that self-heating is triggering the resistive change of VO<sub>2</sub>, as it has been conjectured [10].

Fig. 2c plots the local  $\rho$ , probed inside VO<sub>2</sub>, vs the local  $T$ . It should be noticed that the non Ohmic behavior of  $I - V$  below IMT is fully explained with the interplay between 1)

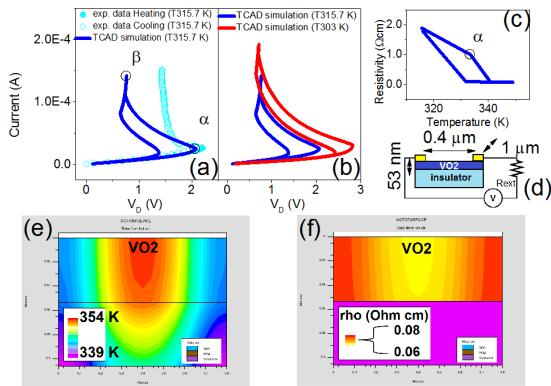


Figure 2. (a) Simulated (blue line) and experimental (cyan symbols)  $I - V$  of VO<sub>2</sub> device. The device has been heated up to 315.7 K by an external heater. (b) Simulated  $I - V$ s at the external temperature  $T$  of 315.7 k (blue line) and of 303 k (magenta line). (c) Local resistivity probed within VO<sub>2</sub>. The IMT switching is highlighted as  $\alpha$  point of  $I - V$  in panel (a) and of resistivity vs temperature in panel (c). (d) Structure of the 2D simulated device. A 53-nm thick VO<sub>2</sub> layer sits on top of an insulator layer. The VO<sub>2</sub> channel length is of 0.4  $\mu\text{m}$ , the channel width is 1  $\mu\text{m}$ . The thermal conductivity of 0.06 W / (cm K) [13] is used in electrothermal simulations. The temperature of the lower boundary of the insulator substrate is set at 315.7 K. (e) Temperature and (f) resistivity 2D plots across the VO<sub>2</sub> layer as extracted in  $\beta$  point of  $I - V$  of panel (a).

self-heating and 2)  $T$ -dependence of  $\rho$ . This results to be in agreement also with experimental findings [14]. Fig. 2e and f are 2D maps of lattice temperature and resistivity, respectively, as extracted in  $\beta$  point of  $I - V$  of Fig. 2a. As it can be seen, the temperature varies across the VO<sub>2</sub> due to Joule heating effect, and this mirrors in a consequent change of the local resistivity (see also Fig. 2c).

The next step is to embed the device physics as provided by the TCAD  $I - V$  into the circuit level simulation of the oscillator at room temperature. To this aim, we simulate  $I - V$  at 303 K (Fig. 2b, red line). It can be observed the impact of the ambient temperature over the  $I - V$ s, especially the voltage and current values at which the IMT occurs. Then, we feed this TCAD  $I - V$  into a Matlab circuit solver tool used to perform the simulation of the oscillator circuit, as it is described in the next section. Our aim is to join up the device level description inside the circuit level simulation (Fig.1).

### C. Oscillator Circuit Simulation

In our beyond-CMOS ONN, the neuron is modeled as a compact relaxation-oscillator made of a VO<sub>2</sub> device in series with a resistor. This highly scalable architecture is shown in Fig.3a and has been validated experimentally [15], [16]. It yields output oscillations at the node  $V_{out}$  for a certain range of supply voltage  $V_{DD}$  and biasing resistor  $R_S$ . The voltage  $V$  applied to the VO<sub>2</sub> device is driven by  $V_{DD}$  and  $V_{out}$  across the output capacitor  $C_P$ . A hysteresis window is defined by the two threshold voltages,  $V_L$  and  $V_H$ , corresponding to the occurrence of MIT and IMT respectively (Fig.3b). To obtain oscillations, the bias current line  $I_L = (V_{DD} - V)/R_S$  must intercept the current  $I$  of the VO<sub>2</sub> device in its hysteresis window. Indeed, it is in this region that a Negative Differential Resistance (NDR) takes place - visible in the  $I - V$  curve when the VO<sub>2</sub> is driven by a current source (Fig.2b) - from which we can form an unstable fixed point to get oscillations.

To simulate the VO<sub>2</sub>-oscillator dynamics, we solve the circuit equation expressed by Kirchhoff's law:

$$C_P \frac{dV}{dt} = I_L - I \quad (1)$$

This first-order differential equation can have oscillatory solutions thanks to the hysteresis relationship between  $I$  and  $V$ . One way to model it at circuit-level is to use a comparator with a positive feedback as in [15]. In this compact model, the comparator continuously stores the time-dependent VO<sub>2</sub> state and switches abruptly when the device voltage  $V$  reaches one of the two thresholds  $V_L$  or  $V_H$ . Hence, it is only near MIT or IMT that the VO<sub>2</sub> resistance varies significantly. Otherwise, the VO<sub>2</sub> resistance is rather constant and is either  $R_{met}$  or  $R_{ins}$ . The dynamics can then be interpreted as simple cycles of RC-charges and discharges. However, TCAD simulations that fit experimental data show a non-linear resistance while VO<sub>2</sub> is in insulator state (right-hand side of Fig.3b).  $R_{ins}$  decreases when  $V$  grows in the hysteresis window, due to the combined effect of 1) self-heating and 2) temperature-dependence of resistivity (Fig. 2c).

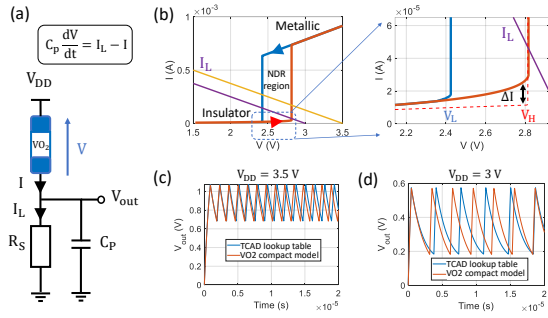


Figure 3. (a) VO<sub>2</sub>-based oscillator with  $R_S = 4 \text{ k}\Omega$  and  $C_P = 500 \text{ pF}$ . (b) VO<sub>2</sub>  $I-V$  curve at 303 K and load lines - yellow:  $V_{DD} = 3.5 \text{ V}$  and magenta:  $V_{DD} = 3 \text{ V}$ . The dashed line is obtained with the compact model [15] and parameters:  $R_{met} = 3.822 \text{ k}\Omega$ ,  $R_{ins} = 246.2 \text{ k}\Omega$ ,  $V_H = 2.818 \text{ V}$ ,  $V_L = 2.424 \text{ V}$ ,  $\alpha = 200$  and  $\tau_0 = 10 \text{ ns}$ . Solid lines are TCAD results:  $I-V$  relationship in insulator state is non-linear. (c) and (d): comparison between oscillatory behavior as generated by the model [15] and through our TCAD approach for  $V_{DD} = 3.5 \text{ V}$  and  $3 \text{ V}$ , respectively. The simulation time-step is 1 ns. In the last example, our method gives different results as  $C_P$ 's discharge slows down before IMT.

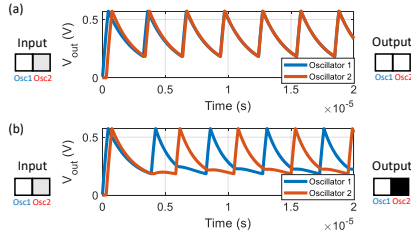


Figure 4. Two oscillators coupled by  $R_C = 10 \text{ k}\Omega$ . Oscillator 2 is turned-on 300 ns after Oscillator 1. They represent pixels for pattern recognition applications - white=in-phase and black=out-of-phase -. a) Simulation using the compact model [15]. b) Using our TCAD method.

To take into account this non-linearity during circuit simulations, we build a Matlab circuit solver that takes as inputs the VO<sub>2</sub>  $I-V$  data from TCAD simulations and the ONN architecture description - number of oscillators, circuit parameters, coupling elements and input signals - (Fig.1). More precisely, we numerically solve (1) by using Euler's method and by keeping track of the VO<sub>2</sub> state. We extract the VO<sub>2</sub> resistance at every time step by interpolating TCAD data stored in a lookup table.

Comparison between our TCAD-based circuit solver and the model [15] are presented for  $V_{DD} = 3.5 \text{ V}$  and  $V_{DD} = 3 \text{ V}$  in Fig.3c and d, respectively. In the first case - yellow load line -, we observe almost no variation between the two approaches. Indeed, if we label  $\Delta I$  the difference between the current extracted with TCAD and the one with the model [15], we have  $I_L \gg \Delta I$  so (1) does not change significantly and there is small discrepancy between the two circuit-solving methods. However, in the second example - magenta load line -  $I_L(V_H) \approx 2 \Delta I(V_H)$  thus  $dV/dt$  is more affected before IMT. This situation is likely to occur as  $I_L$  is generally set as low as possible by increasing  $R_S$  or by decreasing  $V_{DD}$  to minimize the ONN energy consumption. Using our TCAD approach, we predict that the output oscillation slows down

because of the gradual decrease of  $R_{ins}$  in the hysteresis window. Consequently, the ONN computation time - given by multiple oscillation periods - increases along with the energy. Therefore, we believe that the non-linearity in the VO<sub>2</sub> insulator state should be considered for accurate ONN simulation and energy assessment.

To further illustrate the impact of non-linearity in the VO<sub>2</sub> insulator state, we simulate two oscillators coupled by  $R_C = 10 \text{ k}\Omega$  (Fig.4). The second oscillator is turned-on 300 ns after the first one which is 10% of the oscillation period based on the compact model [15]. For a pattern recognition application [16], the two coupled oscillators correspond to a first white pixel and a second light-gray pixel of an input image. Intuitively, we would expect the two oscillators to converge to an in-phase relationship as the compact model [15] predicts (Fig.4a), because the oscillators are initialized with a small delay with respect to the oscillation period. However, by using our TCAD approach we observe the opposite outcome (Fig.4b), i.e the two oscillators converge to an out-of-phase relationship. Hence, considering non-linearity in VO<sub>2</sub> insulator state is key for precise ONN circuit simulation. Finally, we believe our TCAD-based circuit solver is a step toward more robust ONN design and training, as we can also analyze the influence of various factors such as material parameters or ambient temperature.

### III. CONCLUSION

In this work we present an innovative ONN architecture whose basic element, the "neuron", is realized as an oscillator based on vanadium dioxide (VO<sub>2</sub>). Such ONN promises to provide ultra-low power technology for pattern recognition tasks in IoT applications. However, to guide its physical realization a robust design procedure is required. This entails the building of an advanced simulation toolchain (Fig.1) to cover from materials to devices up to circuits, for the assessment of ONN functionality. We show the development of this advanced designing approach with special focus over the VO<sub>2</sub> oscillator. We successfully perform electrothermal simulation of experimental VO<sub>2</sub> devices by customizing the Silvaco TCAD PCM model. In particular, we account the non Ohmic behavior of the  $I-V$  below IMT with the interplay between 1) self-heating and 2)  $T$ -dependence of  $\rho$ . Also, our results support the role of self-heating in driving the phase transition in VO<sub>2</sub>. Then, we feed the TCAD  $I-V$  into a Matlab circuit solver tool to simulate the dynamics of the VO<sub>2</sub> compact relaxation-oscillator. Our simulation approach is able to link the device physics to the circuit level description. Especially, we assess the impact of the non-linearity of resistance in the VO<sub>2</sub> insulator state in the oscillatory behavior, and, in turn, over a proof-of-concept pattern recognition task. Thus, our TCAD-based circuit solver is a first step toward more robust ONN design and training. As future work, we plan to analyze the influence of various factors such as material parameters or ambient temperature over VO<sub>2</sub> oscillator behavior.

## REFERENCES

- [1] J. J. Hopfield, "Neural networks and physical systems with emergent collective computational abilities," *Proc. Natl. Acad. Sci. (USA)*, vol. 79, pp. 2554–2558, 1982.
- [2] E. R. Kandel, J. H. Schwartz and T. M. Jessel, "Principles of Neural Science," 4th ed., McGraw-Hill.
- [3] F. C. Hoppensteadt and E. M. Izhikevich, "Oscillatory neurocomputers with dynamic connectivity," *Phys. Rev. Lett.*, vol. 82, pp. 2983–2986, 1999.
- [4] H. Eslahi, T. J. Hamilton and S. Khandelwal, "Energy-efficient ferroelectric field-effect transistor-based oscillators for neuromorphic system Design," *IEEE J. Explor. Solid-State comput. devices circuits*, vol. 6, pp. 122–129, Dec. 2020.
- [5] P. Maffezzoni, B. Bahr, Z. Zhang, and L. Daniel, "Oscillator array models for associative memory and pattern recognition," *IEEE Trans. Circuits Syst. I Regul. Pap.*, vol. 62, pp. 1591–1598, 2015.
- [6] S. Chen, J. Liu, H. Luo, Y. Gao, "Calculation evidence of staged Mott and Peierls transitions in VO<sub>2</sub> revealed by mapping reduced-dimension potential energy surface," *J. Phys. Chem. Lett.*, vol. 18, pp. 3650–3656, September 2015.
- [7] M. Yang, Y. Yang, B. Hong, L. Wang, K. Hu, Y. Dong, et al., "Suppression of structural phase transition in VO<sub>2</sub> by epitaxial strain in vicinity of metal-insulator transition," *Sci. Rep.*, vol. 6, 23119, March 2016.
- [8] L. Chen, X. Wang, S. Shi, Y. Cui, H. Luo, Y. Gao, "Tuning the work function of VO<sub>2</sub> (100) surface by Ag adsorption and incorporation: Insights from first-principles calculations," *Appl. Surf. Sci.*, vol. 357, pp. 507–517, January 2016.
- [9] A. Haras, M. Witko, D. R. Salahub, K. Hermann, R. Tokarz, "Electronic properties of the VO<sub>2</sub> (011) surface: density functional cluster calculations," *Surf. Sci.*, vol. 491, pp. 77–87, May 2001.
- [10] D. Li, A. A. Sharma, D. K. Gala, N. Shukla, H. Paik, S. Datta and et al., "Joule Heating-Induced Metal–Insulator Transition in Epitaxial VO<sub>2</sub>/TiO<sub>2</sub> Devices," *ACS Appl. Mater. Interfaces*, vol. 8, pp. 1290–12914, 2016.
- [11] J. Dai, X. Wang, Y. Huang, and X. Yi, "Modeling of temperature-dependent resistance in micro- and nanopolycrystalline VO<sub>2</sub> thin films with random resistor networks," *Opt. Eng.*, vol. 47, pp. 1–4, 2008.
- [12] Silvaco "Victory Device User Manual," v. 1.17.4.C, <https://silvaco.com/>, 2020.
- [13] S. Lee, K. Hippalgaonkar, F. Yang, J. Hong, C. Ko, J. Suh, et al., "Anomalously low electronic thermal conductivity in metallic vanadium dioxide," *Science*, vol. 355, pp. 371–374, 2017.
- [14] A. Zimmers, L. Aigouy, M. Mortier, A. Sharoni, S. Wang, K. West et al., "Role of Thermal Heating on the Voltage Induced Insulator-Metal Transition in VO<sub>2</sub>," *Phys. Rev. Lett.*, vol. 110, pp. 056601, 2013.
- [15] P. Maffezzoni, L. Daniel, N. Shukla, S. Datta, and A. Raychowdhury, "Modeling and Simulation of Vanadium Dioxide Relaxation Oscillators," *IEEE Trans. Circuits Syst. I Regul. Pap.*, vol. 62, pp. 2207–2215, Sept. 2015.
- [16] E. Corti, B. Gotsmann, K. Moselund, I. Stolichnov, A. Ionescu, and S. Karg, "Resistive Coupled VO<sub>2</sub> Oscillators for Image Recognition," 2018 IEEE International Conference on Rebooting Computing (ICRC), pp. 1–7, 2018.